



## 저작자표시 2.0 대한민국

이용자는 아래의 조건을 따르는 경우에 한하여 자유롭게

- 이 저작물을 복제, 배포, 전송, 전시, 공연 및 방송할 수 있습니다.
- 이차적 저작물을 작성할 수 있습니다.
- 이 저작물을 영리 목적으로 이용할 수 있습니다.

다음과 같은 조건을 따라야 합니다:



저작자표시. 귀하는 원저작자를 표시하여야 합니다.

- 귀하는, 이 저작물의 재이용이나 배포의 경우, 이 저작물에 적용된 이용허락조건을 명확하게 나타내어야 합니다.
- 저작권자로부터 별도의 허가를 받으면 이러한 조건들은 적용되지 않습니다.

저작권법에 따른 이용자의 권리는 위의 내용에 의하여 영향을 받지 않습니다.

이것은 [이용허락규약\(Legal Code\)](#)을 이해하기 쉽게 요약한 것입니다.

[Disclaimer](#) 

공학석사 학위논문

The Microstructural and  
Mechanical properties of  
platelet (W, M1, M2)C–Co  
Ternary System

2015년 08월

서울대학교 대학원  
서울대학교 대학원  
재료공학부  
바디방가 빠뚜

The Microstructural and  
Mechanical Properties of  
platelet (W, M1, M2)C–Co

# Ternary system

지도 교수 강신후

이 논문을 공학석사 학위논문으로 제출함

2015년 08월

서울대학교 대학원

재료공학부

바디방가 빠뚜

바디방가 빠뚜 의 공학석사 학위논문을 인준함

2015년 08월

위 원 장	박 찬	(인)
부위원장	강신후	(인)
위 원	남기태	(인)

## ABSTRACT

The Microstructural and Mechanical Properties of Platelet

(W, M1, M2) C-Co Ternary System

Pathou Badibanga

Department of Material Science and Engineering

WC-Co cemented carbides are widely used as the material in making cutting tools due to their superior wear resistance, hardness, and toughness. The WC particles that are embedded on the cobalt binder are grown by Ostwald ripening during liquid phase sintering. It has been found that the morphology of WC particles in the cobalt binder consists of platelets, a feature which enhances the material's toughness by deterring crack propagation. By controlling the high energy ball milling, the temperature during reduction, the addition of TiC, the nano effects, and so forth, one can observe the formation of platelet WC.

Until now, the most successful way of controlling the growth of WC grain is with the addition of small amounts of WC grain growth inhibitors. Our previous research on the microstructure evolution of the WC platelet, tungsten carbide particles demonstrated that the morphology, size, and mechanical properties of WC-Co cermets change significantly with the addition of transitional metals such as titanium carbide (TiC), vanadium carbide (VC), and chromium carbide ( $\text{Cr}_2\text{C}_3$ ). Especially in case of TiC, (W,Ti) C-phase was found to have formed with a thin, platelet morphology, enhancing the toughness of the (W,Ti) C-Co cermets.

The purpose of this research was to enhance the hardness of the material by controlling the size and morphology of WC platelets and by maintaining the same toughness for different systems with the addition of NbC to the initial, binary WC-Co system.

In this research, four different ternary systems (such as in-situ, hybrid one and two, and conventional) were prepared using TiC and NbC to control the size and morphology of tungsten carbide platelets. The mole fraction of TiC was fixed at 0.1 in all of the systems, and the NbC mole fraction varied between 0.07 and 0.1 in all of the systems as well. The alloys that started with the oxide powder were produced via planetary milling, and those that started with carbide powder were prepared through ball milling, then all of the systems were sintered at 1450°C for 1 hour. Analysis of the microstructure revealed that all of the systems contained WC platelets and that their aspect ratios had increased when TiC and NbC were added simultaneously. Thus, the addition of transitional metals was found to be effective in increasing the aspect ratios of the different systems that were studied in this research.

주요어 : cemented carbide, platelet, inhibitor effect, ternary system, aspect ratio.

학 번 : 2011-24048

TABLE OF CONTENTS

Abstract.....i  
Table of Contents.....iii  
List of Tables.....v  
List of Figures.....vi

I.  
Introduction.....1  
1. Conventional WC-Co Cermets.....

II. Experimental Procedure.....4

III. Results and Discussion.....7  
1. conventional system.....7  
2. in-situ system.....12  
3. hybrid systems.....17

IV. Summary.....21

V. Reference.....23

VI. Abstract.....

## **LIST OF TABLES**

Table 1. The Size and Manufacturer of Powders

Table 2. The Experimental Procedure of Four Different Systems

Table 3. The Mechanical Properties of the Conventional System Specimens

Table 4. The Mechanical Properties of In-situ System Specimen

Table 5. The Mechanical Properties Comparison between Hybrid 1 and 2 Systems Specimens

Table 6. Solubility in WC (Atomic Fraction)

## **LIST OF FIGURES**

Fig 1. SEM images micrograph of WC-Co and fracture toughness

versus hardness of WC-Co materials comparing nano phase composite samples to conventional composites samples

Fig 2. The morphology change of WC particles in (a).WC-Co, (b). ( $W_{0.9}Ti_{0.1}$ )C-10Co and WC reduced powder

Fig 3. The SEM micrograph of mixed powder via ball milling for 20 hours (conventionally fabricated)

Fig 4. The XRD results of mixed powders and sintered specimens (conventional system)

Fig 5. The SME micrograph of sintered specimens (conventional system)

Fig 6. The SEM micrograph of reduced powder (in-situ system)

Fig 7. The XRD results of reduced powder and sintered specimens (in-situ system)

Fig 8. The SEM micrograph of sintered specimens (in-situ system)

Fig 9. The XRD results of hybrid 1& 2 mixed powder

Fig 10. The SEM micrograph of hybrid 1& 2 mixed powder

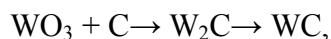
Fig 11. The SEM micrograph of hybrid 1& 2 sintered specimens

Fig 12. The XRD results of hybrid 1& 2 sintered specimens



# I. Introduction

Having begun in Germany during the First World War, cemented carbides (WC-Co), a mixture of tungsten carbide powder with a cobalt metallic binder, were first issued in 1923. The term “cemented” refers to the tungsten carbide particles being captured in a metallic binder and grown by Ostwald ripening during liquid phase sintering [1]. The morphology of the WC particles in a cobalt binder is a truncated, triangular prism, and there are also some WC platelets present (see Fig 1.a) [2, 3]. The formation of platelets has been reported to occur by 1) the dissolution and reprecipitation of mechanically alloyed WC-Co or WC-TiC-Co (Meadows-Shatov route) and 2) the dissociation of  $\text{Co}_3\text{W}_3\text{C}$  and growth of WC in a Co binder. But in recent research, it has been observed that WC platelets are formed during carbothermal reduction (Fig 2.c) without a cobalt binder, which is essential for being the medium for the mass transfer of WC particles in the process. WC can be synthesized according to the sequence of



and WC changes its morphology from an irregular shape to a platelet shape in the temperature range of 1200 to 1300°C during the carbothermal reduction process [4].

Generally, cemented carbides are a group of sintered materials with outstanding properties such as superior wear resistance, hardness,

and toughness [5, 6]. As a result, these materials have a wide range of industrial applications, particularly in the tool-cutting industry. More than approximately 75% of all cemented carbide cutting tools are based on tungsten carbide [7]. WC-Co materials have excellent performance and outstanding mechanical properties over a broad range of applications [8, 9], as is shown in (Fig 1.b). The exceptionally high hardness of this material is achieved through its microstructure of superfine grain. Data shows that the fracture toughness of sintered WC-Co using nano powder decreases as the hardness increases [10]. With the development of various toughening methods for ceramic materials such as transformation toughening [11] and whisker reinforcement [12], the strength and fracture toughness of ceramic materials have been improved significantly, but researchers in this field continue to work to extend the material's service life, hardness, and strength as well as the wear resistance, for example by the addition of transitional carbides. [2, 13]

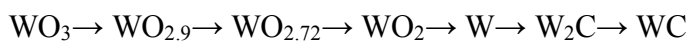
Some previous research on the microstructure evolution of platelets demonstrated that the morphology, size, and mechanical properties of a WC-Co cermet changes significantly with various additives such as vanadium carbides (VC) [14, 15] and titanium carbides (TiC) (see Fig 2.b), resulting in new microstructures that consist of thin, tungsten carbide platelets embedded in the cobalt phase,

thus enhancing the material's toughness by deterring crack propagation [16]. The objective of this research is to understand the effect of the addition of NbC to the microstructure and to understand the properties of WC platelet formation in (W,Ti)C, as well as the general microstructure, the ability to sinter it, and the toughness of the system.

## II. Experimental Procedure

The manufacturers and the specifications of the powders that were used in this study are listed in Table 1 in the appendix. All of the carbide and oxide powders were micro-sized. While preparing the in-situ, conventional, and hybrid systems, this study used differently sized, raw powders that are manufactured by Sigma Aldrich and Nanotec. The powders were mixed together to reach the different target compositions of  $(W_{1-x}Ti_{0.1}Nb_x)C$  for the in-situ system,  $WC-3.3TiC-xNbC$  for the conventional system,  $(W_{0.9}Ti_{0.1})C-xNbC$  for the first hybrid system, and  $(W_{1-x}Nb_x)C-3.3TiC$  for the second hybrid system, with the mole fraction,  $x$ , varying between 0.07 and 0.1.

The mixtures of oxide were milled using a planetary mill (Fritsch Pulverisette 7, Germany) with tungsten carbide balls. All of the milling process was conducted at a speed of 250 rpm, for a period of twenty hours. The ball-to-powder weight ratio was fixed at 40:1. The initial  $WO_3$  and graphite materials changed according to the transformation of



during the carbothermal reduction. [21, 22] Generally, the WC that is obtained from synthesized oxide and graphite is formed absolutely at a temperature over  $1600^{\circ}C$  [23]. It has been shown in the separate research that the synthesizing of  $WO_3$  and graphite to produce WC can

be done at low temperatures due to the high-energy, ball milling effect. High-energy milling affects the raw powder by causing dislocation, vacancy, and a large amount of defects in the powder. So, because of the excess energy from the breaking down of the material, reduction at a low temperature is also possible [24]. Thus, the high-energy ball milling resulted in increasing the defect density and in decreasing the reduction temperature.

The milled powders were sieved, using a 125 mesh-sized sieve, to remove agglomerates. The final powders were produced in carbothermal reduction at 1400°C for two hours in a graphite furnace under a vacuum. The reduced powder was mixed with 10wt% by weight cobalt binder in ethanol via horizontal ball milling for twenty hours and then was dried for twenty-four hours in an oven at 100°C.

As for the conventional powder, it was mixed via ball milling for a period of twenty hours, also using horizontal ball milling, and was dried for twenty hours in the oven at 100°C. The dried powder was then mixed with 10wt% by weight cobalt binder in ethanol via horizontal ball milling for twenty hours and was dried again for twenty four hours in an oven at 100°C.

The powders from all four systems were compacted into discs under a pressure of 150 MPa, and the compacted materials were sintered at 1450°C for one hour in a graphite furnace. We used X-ray

diffraction (the XRD: Rigaku D-Max2500 diffractometer, which uses Cu K $\alpha$ ,  $\lambda=1.54056\text{\AA}$ , as a source of radiation and a rotating anode) to characterize the phase and a scanning electron microscope, SEM (JSM-6360, JOEL), to analyze the microstructure and phase. We polished our specimens to between 6 and 1  $\mu\text{m}$  with a diamond slurry before the analysis. Finally, the mechanical properties of the sintered cermets were obtained from the Vickers hardness measurement by analyzing the length of cracks, which emanated from the corners of the Vickers hardness indentation.

### **III. Results and Discussion**

#### **1. Conventional system**

Carbide powders, such as WC, TiC, NbC, and Co, that are manufactured by nanotech were milled via ball milling in ethanol for twenty hours to mix up the powder. This milling process—with no strain effect—resulted in an agglomerates powder with an equiaxed-shaped structure as displayed in the SEM results displayed in Figure 3. Which shows the result of two different systems binary and ternary. The ternary system WC-3.3TiC-4.2NbC was designed to observe the effect of NbC on the WC-3.3TiC binary system. Niobium carbide can be used to inhibit WC grain growth in hardmetal as reported in the different study. But after investigation by the SEM it was find that the addition of NbC transitional metal into WC-3.3TiC binary system was less effective in inhibiting the WC grain as shown in the SEM results.

Figure 4 shows the XRD results for the powder and sintered specimens of binary and ternary systems:

a) the XRD results of the mixed powder via ball milling in ethanol for twenty hours and

b) the XRD results of sintered specimens at 1450°C for one hour.

The X-Ray powder diffraction (XRD), is an instrumental technique that is used to identify crystalline materials, is an important technique because it is non-destructive, non-contrast, fast and sensitive. XRD however does not provide the quantitative compositional data obtained by SEM. The objective of an X-Ray diffraction is the measurement to determine the dimensions and shape of unit cell and to identify the detailed structure of the molecule.[32].

The initial powders for the WC-3.4TiC binary system were hexagonal WC and cubic TiC, while the initial power for the WC-3.4TiC-4.2NbC and WC-3.4TiC-6.1NbC ternary systems were cubic TiC, cubic NbC and hexagonal WC. The XRD results of the WC-3.4TiC powder mixed via ball milling in ethanol, which has an equiaxed powder morphology in the previously displayed SEM results, indicate a hexagonal-closed pack with a WC peak with some TiC peaks. As a result of mixed powders with no reduction process and no strain effect, there was no formation of a solid solution, as indicated in the diffraction pattern. Since there is almost no Ti solubility predicted in WC up to 2000C as displayed in WC-TiC binary phase diagram show in the figure 13. Some research also say that solubility of different transitional metals in



WC in cemented carbides at around 1700k are as follow: Ta had the highest solubility, followed by Nb, Cr and V, all with atom fraction in the  $10^{-3}$  range. Ti and Mn show lower solubilities in the  $10^{-6}$  or  $10^{-5}$  range. Zr and Co solubility are too lower. [33] as displayed in the table 6

According to my result there were also no peak shifting in the diffraction patter of the binary system.

Both of the ternary systems, WC-3.4TiC-4.2NbC and WC-3.4TiC-6.1NbC, have a WC peak at 31.51, 35.64, and 48.30 for the (001), (100), and (101) peaks respectively as indicated by the JCPDS diffraction angles  $2(\theta)$  of standard WC. The ternary systems didn't also show any peak shifting, proving that the solid solution didn't formed. The XRD results of all of these three compositions did not show any peak broadening, giving a stronger proof that the crystallite size of the powders was bounded in a micro-size range.

Figure 4.b, exhibits the XRD results of the three different sintered specimens. After mixing WC-3.4TiC, WC-3.4TiC-4.2NbC and WC-3.4TiC-6.1NbC with 10wt% Co, the materials were sintered at 1450°C for one hour in a vacuum. The (001), (100), and (101) peaks of the three sintered specimens shifted towards a high angle differently from the powder diffraction patterns that did not shift as indicating by the JCPDS diffraction  $2(\theta)$  of standard WC, signaling that a solid

solution had formed and indicating a reduction in the lattice spacing that had occurred during the sintering process. More research are need in order to understand the formation of solid solution during the sintering process of the specimen. The SME analysis of the two specimens revealed that the equiaxed WC carbide appeared uniformly dispersed throughout the Co, (Ti,W)C, and (Ti,W,Nb)C in respect to each specimen. As displayed in Figure 5, the equiaxed shape of the WC grain is the result from not using both high-energy ball milling and carbothermal reduction in the production process, as demonstrated in previous paragraph. The formation of the microstructure appears to be a more solid solution with an increase in the NbC content. Also, the WC grain quantity decreases in the cobalt binder as the NbC content increases. The equiaxed WC grain exhibits more coursing with the addition of NbC. In the image, the gray equiaxed grain is the WC, and the dark background color is one of the (Ti,W)C, (Ti,W,Nb)C and Co binders.

The mechanical properties of the sintered cermets are listed in Table 1. The hardness and toughness values were respectively obtained through the Vickers measurement and the indentation technique, using a 30 kgf load. The hardness and the toughness of

WC-3.4TiC-10 wt%Co,

WC-3.4TiC-4.2NbC-10 wt%Co,

and WC-3.4TiC-6.1NbC-10 wt%Co  
ranged between 14 to 15 GPa and 12 to 13 MPa<sup>1/2</sup>. The porosity of the  
sintered body is at a good level of A1B1, suggesting that the sintering  
of the specimens had finished well.

## **2. in-situ**

The in-situ system which started with oxide powders WO<sub>3</sub>, TiO<sub>2</sub>,

$\text{Nb}_2\text{O}_5$  and graphite were milled and reduced at  $1400^\circ\text{C}$  for 2 hours in the graphite furnace. High energy milling results in a high amount of defect, dislocation and vacancy in the raw materials facilitating the rapid reduction at low temperature.

As observed in figure 6, different compositions:  $(\text{W}_{0.9}\text{Ti}_{0.1})\text{C}$ ,  $(\text{W}_{0.83}\text{Ti}_{0.1}\text{Nb}_{0.07})\text{C}$  and  $(\text{W}_{0.8}\text{Ti}_{0.1}\text{Nb}_{0.1})\text{C}$  are prepared to see the effect of NbC content on the powder morphology change. Figure 6.(a) shows the microstructure of  $(\text{W}_{0.9}\text{Ti}_{0.1})\text{C}$  which displays the platelet formation in it. It was not easy to find evidence of platelet formation in  $(\text{W,Ti})\text{C}$  powder, however, the platelet WC was found to form during powder synthesis and in the early stage of sintering in the  $(\text{W,Ti})\text{C}$  systems, but as NbC content increases, the formation tendency of WC platelet carbide decreases. The (101) prism plane develops preferentially in the  $(\text{W}_{0.9}\text{Ti}_{0.1})\text{C}$ , which serves as a base for thin platelet morphology. In a separate research [25], it has been reported that WC forms between  $600$  and  $800^\circ\text{C}$  from milled powder of  $\text{WO}_3$  and C, while TiC forms about  $100$  and  $1200^\circ\text{C}$  from milled mixtures of  $\text{TiO}_2$  and C. therefore it is more likely that WC is expected to form first at low temperature and followed by the  $(\text{Ti,W})\text{C}$  formation between  $1000$  and  $1200^\circ\text{C}$ . This view is supported by the XRD results in figure [?] which demonstrates the co-existence of  $(\text{Ti,W})\text{C}$  and  $(\text{W,Ti})\text{C}$  [7].

In fcc  $(\text{Ti}_{1-x}\text{W}_x)(\text{CN})$  ceramic systems, it has been reported that the

WC phase forms together with the (Ti,W)(CN) phase when the mole fraction,  $x$ , exceeds 0.3. the morphology of WC from (Ti,W)(CN) also consists of thin platelet with similar aspect ratio to that of (W,Ti)C. the WC platelet formation is further facilitated in the presence of nitrogen[26]. The most common crystal shape of WC in the WC-Co system is truncated trigonal prism, and the shape of WC is known to be sensitive to the binder content and the composition [27, 28] the formation of platelet morphology was attributed to the high anisotropy in surface energy and growth kinetics with respect to crystallographic planes, which are yet to be determined [7]. In fact, WC is thermodynamically less stable than TiC and Ti (CN) and (Ti,W)C and WC tends to dissolve and precipitate readily in the system [29.30]. The free energy of formation of TiC and WC are -162 and -34Kj/mol, respectively at 1700K [31]. Therefore during the sintering process, (W,Ti)C is expected to dissolve preferentially due to its lower thermal stability compared to (Ti,W)C , even if it is the major phase of the system with regards to volume . the (W,Ti)C phase that is dissolved in the liquid Co precipitates and grows on preferred planes of remaining (W,Ti)C.

As reported in a previous study [28], binder content and composition are known to influence the extent of the anisotropy in the surface energy of WC. Platelet [26]. However the present research

shows that the presence of Co is not a direct cause for the WC platelet formation as seen from the figure 6(a) does clearly demonstrate that ordinary thin platelet formation is more apparent in the (W,Ti)C-Co system.

The preliminary study indicates that the formation of WC platelets during powder synthesis is strongly affected by the powder reduction temperature, content of solute in (W,M)C and binder contents. This implies that factors that promote phase separation and anisotropy might also control the formation of thin platelets these factors include solubility limit, the thermal stability of the phase, possible strains developed in the system and the interfacial energy of carbide in liquid binder.

Niobium carbide is an extremely hard refractory ceramic material frequent additive in cemented carbides. NbC is selected in this study due to its hardness (19.6GPa) and high melting temperature (3600C). It was found in this study that NbC addition decreases the grain size of ultrafine WC particles, the formation tendency of WC platelet carbide decreases as displayed in figure 6(b) & (c). Meanwhile, adding NbC decrease the volume fraction of Co phases of the alloys thus increases the fracture toughness of the alloys

The in-situ system which started with oxide powders  $\text{WO}_3$ ,  $\text{TiO}_2$ , and  $\text{Nb}_2\text{O}_5$  were milled and then underwent reduction for two hours in a

graphite furnace. The antecedent high-energy milling resulted high amounts of defects, dislocation, and vacancy in the raw materials, so as to facilitate the rapid reduction at the low temperature at 1400°C.

As can be seen in the Figure 7, the different compositions of

a)  $(W_{0.9}Ti_{0.1})C$ ,

b)  $(W_{0.83}Ti_{0.1}Nb_{0.07})C$ , and

c)  $(W_{0.8}Ti_{0.1}Nb_{0.1})C$

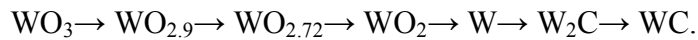
show the resulting effect of the NbC content on the changes in the powder morphology. According to Figure 6.a, the microstructure reveals that an agglomeration of WC platelet particles had developed, as the NbC content increased and the tendency for the formation of WC platelet carbides decreased, a result that is seen in Figures 6.b and 6.c. The formation of the WC platelet carbides is attributed to the combined effects of the high-energy milling, the reduction temperature, and the addition of a secondary, transitional metal carbide.

The diffraction patterns in Figure 7, display the results of the three different solid solution systems:  $(W_{0.9}Ti_{0.1})C$ ,  $(W_{0.83}Ti_{0.1}Nb_{0.07})C$ ,

and  $(W_{0.8}Ti_{0.1}Nb_{0.1})C$ . The major WC peak in all of these three systems did not show any sign of shifting.

The  $(Ti,W)C$  solid solution formed in the  $(W_{0.9}Ti_{0.1})C$  binary system, and the  $(Ti,W,Nb)C$  solid solution formed in both ternary systems. There was a  $W_2C$  phase also present in the ternary system, which is a result from the lack of carbon during the reduction process.

The XRD analysis of the sintered specimen with 10%wtCo revealed that there had been a shift in the major WC peaks to a higher angle, meaning that lattice spacing decreased and that it had caused the formation of a solid solution. Additionally, the  $W_2C$  phases that were present in the XRD analysis of the powder were all transformed into WC, a process that is explained in another study that shows how  $WO_3$  raw material changes through carbothermal reduction from [10]-[11]



In this way, the disappearance of  $W_2C$  is attributed to the setting of the high temperature during the sintering process

The microstructures of the different sintered samples were obtained from the high-energy ball milling powder. The samples exhibited WC platelets,  $(TiW)$ , and  $(Ti,W,Nb)C$  dispersed in the cobalt binder. The four systems were

a) WC-Co,

b)  $(W_{0.9}Ti_{0.1})C$ -10Co,



c)  $(W_{0.83}Ti_{0.1}Nb_{0.07})C$ , and

d)  $(W_{0.8}Ti_{0.1}Nb_{0.1})C-10Co$ .

The WC platelets in the WC-Co system had a low aspect ratio and also indiscrete WC powder boundaries. The addition of a 0.1 mole fraction of TiC caused discrete WC powder boundaries and an increase in the aspect ratio. Also, when the 0.07 to 0.1 mole fraction of NbC was added to the binary system, the aspect ratio of the specimen increased much more, resulting in the increased hardness of the samples. Compared to the conventional system, the in-situ system resulted in an improvement to the material's hardness; but on the other hand, it had a slight decrease in the toughness.

### **3. Hybrid Systems**

Figure 9, shows the XRD results of hybrid systems 1 and 2. The

result of the first hybrid system is derived from a solid solution of  $(W_{1-x}Ti_{0.1})C$  powder that is milled and reduced at  $1400^{\circ}C$  for two hours. After these steps, the material was then mixed with an NbC carbide powder via ball milling in ethanol for twenty hours. During the analysis of the final material, the diffraction patterns indicated two different peaks. There was a WC and  $(Ti,W)C$  solid solution in the binary system, that is the one of  $(W_{0.9}Ti_{0.1})C$ . However, the ternary systems,  $(W_{0.9}Ti_{0.1})C-4.2NbC$  and  $(W_{0.9}Ti_{0.1})C-6.1NbC$ , indicate that a single phase, hexagonal-closed pack WC had formed in all of the subsequent cases.

The  $W_2C$  phase was also observed in both ternary systems. Again, the formation of  $W_2C$  is attributed to the duration of the carbothermal reduction as explain above. A NbC peak is also present in the diffraction patterns of the ternary systems,  $(W_{0.9}Ti_{0.1})C-4.2NbC$  and  $(W_{0.9}Ti_{0.1})C-6.1NbC$ . The JCPDS diffraction angles  $2(\theta)$  of standard WC did not indicating any peak-shifting. The SME microstructure of the mixture powder resulted in the agglomeration of nano-crystallite carbides. The extent of agglomeration is found to increase with the Ti content [3]. After mixing  $(W_{0.9}Ti_{0.1})C$ ,  $(W_{0.9}Ti_{0.1})C-4.2NbC$ , and  $(W_{0.9}Ti_{0.1})C-6.1NbC$  with 10wt% Co and after sintering it at  $1450^{\circ}C$  for one hour, the WC carbide appeared uniformly distributed and appeared as thin platelets, a finding that is reflected in figure 8. The

EDS analysis confirmed that the gray-colored phase is the pure WC and that the black background is the (Ti,W)C and the cobalt binder for the (W<sub>0.9</sub>Ti<sub>0.1</sub>)C-10 wt%Co and is the (Ti,W,Nb)C and cobalt for (W<sub>0.9</sub>Ti<sub>0.1</sub>)C-4.2NbC-10 wt%Co and (W<sub>0.9</sub>Ti<sub>0.1</sub>)C-6.1NbC-10 wt%Co. This morphology differs with that which was found in the conventional system, as shown in figure 5, which has an equiaxed shape. The microstructure is same with that which is seen in the in-situ system. However the aspect ratio increases with the addition of TiC into the WC-Co and increases even more with the addition of NbC in the (W<sub>0.9</sub>Ti<sub>0.1</sub>)C-10 wt%Co. This is attributed to the inhibiting effect of TiC and NbC on the growth of WC.

The result of the second hybrid system was produced from solid solution of (W<sub>1-x</sub>Nb<sub>x</sub>)C that was crushed by high-energy ball milling and then reduced at 1400°C for two hours before being mixed with 3.3TiC powder via ball milling for twenty hours. This system consisted also of a binary system, WC-3.3TiC, and also a ternary system, (W<sub>0.93</sub>Nb<sub>0.07</sub>)C-3.3TiC and (W<sub>0.9</sub>Nb<sub>0.1</sub>)C-3.3TiC. The XRD analysis of the binary system, WC-3.3TiC, which was a mixture of WC and TiC carbide powder through ball milling, resulted in separate WC, W<sub>2</sub>C, and TiC peaks. In the ternary systems, (W<sub>0.93</sub>Nb<sub>0.07</sub>)C-3.3TiC and (W<sub>0.9</sub>Nb<sub>0.1</sub>)C-3.3TiC, the results indicated the presence of four peaks: WC, W<sub>2</sub>C, TiC and (Nb,W)C of solid solution. The SEM results for

the powders of the three systems (the binary system WC-3.3TiC and the ternary systems  $(W_{0.93}Nb_{0.07})C$ -3.3TiC and  $(W_{0.9}Nb_{0.1})C$ -3.3TiC) resulted also in agglomeration of nano-crystallite carbides, and the size of crystallites seems to be the same. The SEM results of the sintered specimens of those systems showed the same microstructure consisting of WC platelets. This finding confirms that the mechanical properties of WC-Co alloys could vary, depending on the platelets. The hardness and density of the material increase as the aspect ratio increases. In light of the microstructures that were produced and the results that were obtained from the mechanical tests, the second hybrid system showed a greater increase in hardness compared to the first hybrid system.

## **IV. Summary**

In this research, four different systems were investigated in

order to discover the effectiveness of NbC inhibitors on a WC-TiC-Co binary system. The microstructures and mechanical properties of various (W,Ti,Nb)C-Co systems were investigated. In relation to the function of NbC on the contents, the aspect ratio of the WC particles was also affected by the addition of NbC. The average particle size of WC decreased with the addition of NbC, and the decreased aspect ratio of WC particles caused an increase in the hardness, though the fracture toughness decreased.

The in-situ system, which underwent reduction and then sintering, resulted in WC platelet with a high aspect ratio, an effect that increased the hardness of the system. On the other hand, its toughness was measured to be lower than compared to the conventional system.

It was confirmed in this research that high-energy milling and the addition of TiC both contribute to the formation of WC platelets during the carbothermal reduction process. Also, NbC seems to also inhibit grain growth. More research is necessary in order to maintain the toughness of a ternary system

## REFERENCES

- [1] H. E. Exner, Physical and chemical nature of cemented carbides. International Metals Reviews, 1979. 4. p. 149-173
- [2] Z. Zak Fang\*, Xu Wang, Taegong Ryu, Kyu Sup Hwang, H.Y. Sohn, Synthesis, sintering, and mechanical properties of nanocrystalline cemented tungsten carbide-A review, International Journal of Refractory Metals and Hard Materials, 2009. 27. p.288-299
- [3] S. Ilay<sup>a</sup>, C.H. Allibert<sup>a\*</sup>, M. Christensen<sup>b</sup>, G. Wahnström<sup>c</sup>, Morphology of WC grains in WC-Co alloys, Materials Science and Engineering 2008.A486 p.253-261
- [4] Jinmyung Kim Seoul National university graduate School thesis, 2012
- [5] Osung Seo and Shinhoo Kang, On the Dissolution of WC in WC-Co Alloys, Key Engineering Materials 2006. Vols.317-318 p. 263-266
- [6] Guan-Jun Yang, <sup>a</sup>Pei-Hu Gao, <sup>a,b</sup>Cheng-Xing Li<sup>a</sup> and Chang-Jiu Li<sup>a,\*</sup> Simultaneous strengthening effects in WC-(nanoWC-Co) Scripta Materiala. 2012.66. p. 777-180
- [7] Hyomon Nam, Jaehyuk Lim, Shinhoo Kang, Microstructure of (W,Ti)C-Co system containing platelet WC, Materials Science and Engineering 2010. A 527. p. 7163-7167
- [8] Gwan-Hyoung Lee, Shinhoo Kang, Sintering of nano-sized WC-Co powders produced by a gas reduction-carburization process, Journal of

Alloys and compounds. 2006.419. p.281-289

[9]. S.G. Huang <sup>a</sup>, K. Vanmeensel<sup>a</sup>, L. Li <sup>b</sup>, O. Van der Biest <sup>a</sup>, J. Vleugels <sup>a,\*</sup> Tailored sintering of VC-doped WC-Co cemented carbides by pulsed electric current sintering, International Journal of Refractory Metals and Hard Materials. 2008.26. p.256-262

[10] Z. Zak Fang\*, Xu Wang, Taegong Ryu, Kyu Sup Hwang, H.Y. Sohn International Journal of Refractory Metals and Hard Materials

[11] J.F. Yang, T. Ohiji, T. Sekino, Phase transformation, microstructure and mechanical properties of Si<sub>3</sub>N<sub>4</sub>/SiC composite, Journal of the European Ceramic Society 2001.2. p. 2179-2183

[12] K. Gen, W.J. Lu, Y.X. Qin, D. Zhang, Materials Research Bulletin 2004 P. 873-879

[13] S.G. Huang <sup>a</sup>, L. Li <sup>b</sup>, K. Vanmeensel <sup>a</sup>, O. Van der Biest <sup>a</sup>, J. Vleugels <sup>a,\*</sup> VC, Cr<sub>3</sub>C<sub>2</sub> and NbC doped WC-Co cemented carbides prepared by pulsed electric current sintering International Journal of Refractory Metals and Hard Materials. 2007. 25. p. 417-422

[14] Y. Morisada, Y.Miyamoto, SiC-coated carbon nanotubes and their application as reinforcements for cemented carbides, Materials Science and Engineering 2004.A381. p. 57-61

[15] Z. Qiao, X.-F.Ma, W.Zhao, H.-G. Tang, S. Cai, B.Zhao, Fabrication, microstructure and mechanical properties of novel cemented hard alloy

obtained by mechanical alloying and hot-pressing sintering, Materials Science and Engineering 2007.A460M461 p. 46-49

[16] Hyoung R. Lee and Deug J. Kim, Nong M. Hwang and Doh- Yeon Kim, Role of Vanadium Carbide Additive during Sintering of WC-Co: Mechanism of Grain Growth Inhibiting, Journal of American Society 2003. 86[1] p. 152-154

[17]. Jonathan Weidow\*, Hans-Olof Andrén, Grain and phase boundary segregation in WC-Co with small V, Cr or Mn additions, Acta Materialia. 2010.58. p. 3888-3894

[18] Osung Seo<sup>1,a</sup> and Shinhoo Kang<sup>2,b</sup>, Key Engineering Materials 2006. P.263-266

[19] Bonache, V., Salvador, M., Busquets, D., Burguete, P., Martinez, E., Sapiña, F., Sánchez, E. international journal of refractory Metals and Hard Materials 2011

[20] Lay, S., Loubradou, M., Schubert, W. d. Journal of the American ceramic Society 2006

[21] Liu, W., at al., Materials Chemistry Physics. 2008 P.235-240

[22] Jin, Y., at al., powder Technol. 2011 P.482-485

[23] Toth, L.E., Transitional carbides and nitrides Vol. 1971 Academic press New York

[24] park, S. and S. Kang, Toughened ultra-fine (Ti,W)(CN)-Ni cermets Scripta Materials., 2005.52. p. 129-133



- [25] H. Kwon, S. Kang, Effect of milling on the carbothermal reduction of oxide mixture for (Ti,W)C-Ni, Materials Transaction, JIM 2008 1594-1599
- [26] Y.J. Kang, S. Kang, WC-reinforced (Ti,W)(CN), Journal of European Ceramic Society. 2010.30. p. 793-798.
- [27] S. Lay, C.H. Allibert, M. Christensen, G. Wahnström, Morphology of WC grains in WC-Co alloys, Materials Science and Engineering 2008.A486. p. 253-261
- [28] D-B. Lee, K.-W. Chae, Journal of the Korean Chemical Society. 2004 P.131-135
- [29] S.Y. Ahn, S. Kang, Formation of core/rim structures in Ti(C,N)-WC-Ni cermets via dissolution and precipitation process, Journal of American Ceramic Society 2000 P. 1489-1494
- [30] S. Ahn, S. Kang, Dissolution phenomena in the Ti(C<sub>0.7</sub>N<sub>0.3</sub>)-WC-Ni system, International Journal of Refractory Metal and Hard Materials. 2008.26. p. 340-345
- [31] M.W. Chase et al. (Eds.), JANAF Thermochemical Tables, 3<sup>rd</sup> ed., Journal of Physical and Chemical Reference Data 14(1985).
- [32] Ruhee Hussain and H.D. Juneja International journal of Chemical Science 2009.7(2).p. 632-638
- [33] Jonathan Weidow, Sven Johansson, Hans-Olof Andrén, and Göran Wahnström, journal of the American Ceramic Society

## Tables

Table 1. Manufactures and specification of the powders used in this research

Powder	Size( $\mu\text{m}$ )	Manufacturer	Powder	Size( $\mu\text{m}$ )	Manufacturer
$\text{WO}_3$	$\leq 20$	Aldrich	WC	2.73	Nanotech
$\text{TiO}_2$	40	Aldrich	TiC	1.35	Nanotech
$\text{Nb}_2\text{O}_3$	40	Aldrich	NbC	1.45	Nanotech
C	1.7	Lonza			
Co	2.3		Co	2.3	Nanotech

Table 2. Experimental procedure of four different systems used in the research

In-situ ( oxide)	Hybrid 1 (oxide + carbide)	Hybrid 2 (oxide + carbide)	Conventional ( carbide)
$(W_{1-x}Ti_xNb_x)C-10wt\%Co$	$(W_{0.9}Ti_{0.1})C-xNbC-10wt\%Co$	$(W_{1-x}Nb_x)C-3.3TiC-10wt\%Co$	$WC-3.3wt\%TiC-xNbC-10wt\%Co$
High energy ball milling at 250 rpm for 20hrs			×
Sieving with 125 mesh to remove agglomerate			
Carbothermal reduction at $1400^{\circ}C$ for 2hrs			×
Ball milling (90wt%carbide +10wt%Co) in ethanol at 200rpm for 20hrs			
Sintering at $1450^{\circ}C$ for 1h			
Grinding (#120, #600) & polishing (1/ $\mu m$ , 6/ $\mu m$ )			
Phase & morphology identification (XRD, SEM & Optical microscopy)			

Table 3. The mechanical properties of the conventional system specimens

Specimens	Hardness (GPa)	Toughness (MPa <sup>1/2</sup> )	Porosity level
WC-3.4TiC-10wt%Co	14.39	13.84	A1B1
WC-3.4TiC-4.2NbC-10wt%Co	15.20	12.63	A1B1
WC-3.4TiC-6.1NbC-10wt%Co	15.30	13.59	A1B1

Table 4. Mechanical properties of in-situ system specimens

Specimens	Hardness (Gpa)	Toughness (MPa <sup>1/2</sup> )	Porosity level
(W <sub>0.9</sub> Ti <sub>0.1</sub> )C-10wt%Co	14.70	12.77	A1B2
(W <sub>0.88</sub> Ti <sub>0.1</sub> Nb <sub>0.02</sub> )C-10wt%Co	17.23	12.30	A1B1
(W <sub>0.8</sub> Ti <sub>0.1</sub> Nb <sub>0.1</sub> )C-10wt%Co	17.68	11.67	A1B1

Table 5. The mechanical properties comparison between Hybrid 1& 2

systems

Specimens	Hardness (Gpa)	Toughness (MPa <sup>1/2</sup> )	Porosity level
(W <sub>0.9</sub> Ti <sub>0.1</sub> )C-10Co	14.12	12.66	A1B2
(W <sub>0.9</sub> Ti <sub>0.1</sub> )C-4.2NbC-10Co	15.61	11.80	A2B1
(W <sub>0.9</sub> Ti <sub>0.1</sub> )C-6.1NbC-10Co	15.72	11.80	A1B1
WC-3.3TiC-10Co	14.19	11.77	A1B2
(W <sub>0.9</sub> Nb <sub>0.07</sub> )C-3.3TiC-10Co	15.20	11.50	A1B2
(W <sub>0.9</sub> Nb <sub>0.1</sub> )C-3.3TiC-10Co	16.72	11.40	A1B1

Table 6. Solubility in WC (Atomic Fraction) [33]

<b>Table IV. Solubility in WC (Atomic Fraction)</b>			
	Experiments	Theory—reference state: second solid state	Theory—reference state: dissolved in binder
Ti	$(1.9 \pm 0.3) \times 10^{-5}$	$1.3 \times 10^{-5}$	
V	$(1.60 \pm 0.07) \times 10^{-3}$	$4.3 \times 10^{-3}$	$8.9 \times 10^{-4}$
Cr	$(1.84 \pm 0.09) \times 10^{-3}$	$1.0 \times 10^{-2}$	$5.3 \times 10^{-4}$
Mn	$(9 \pm 2) \times 10^{-6}$		
Co	$< 9 \times 10^{-6}$	$3.5 \times 10^{-7}$	
Zr	$< 3 \times 10^{-5}$	$1.2 \times 10^{-8}$	
Nb	$(6.1 \pm 0.2) \times 10^{-3}$	$1.4 \times 10^{-3}$	
Hf		$5.7 \times 10^{-8}$	
Ta	$(9.59 \pm 0.09) \times 10^{-3}$	$2.3 \times 10^{-3}$	

## FIGURES

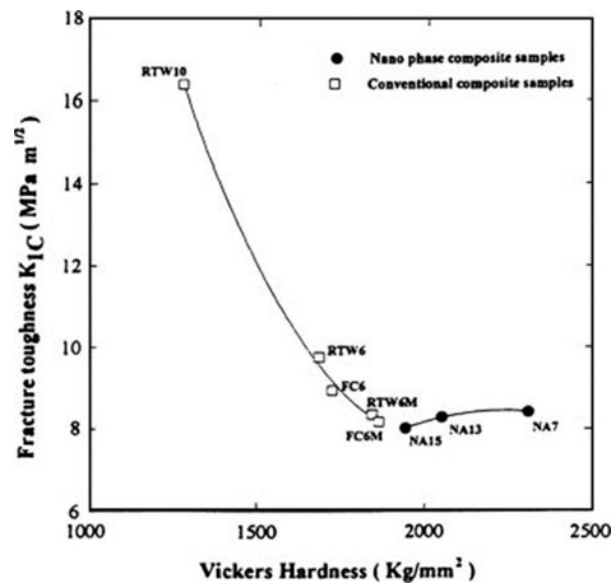
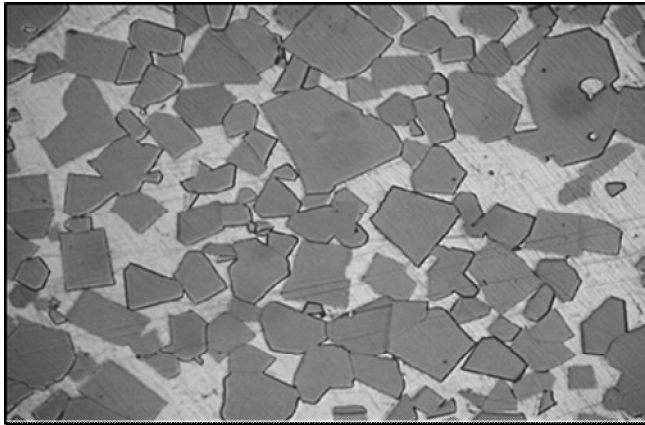


Fig 1. SEM image micrograph of WC-Co (a) reprinted by reference 10 and fracture toughness versus hardness of WC-Co materials comparing nano phase composite samples to conventional composites samples (b) reprinted by reference 15.



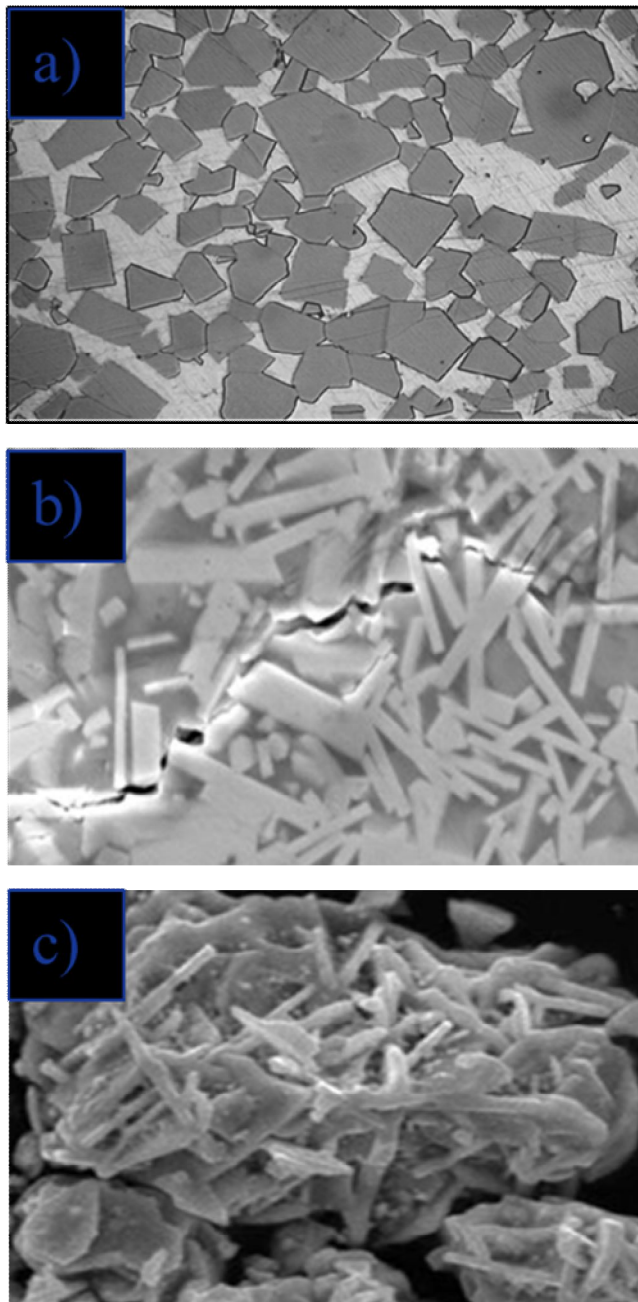


Fig 2. The morphology change of the WC particles in (a).WC-Co, (b).  $(W_{0.9}Ti_{0.1})C$ -10Co and WC reduced powder

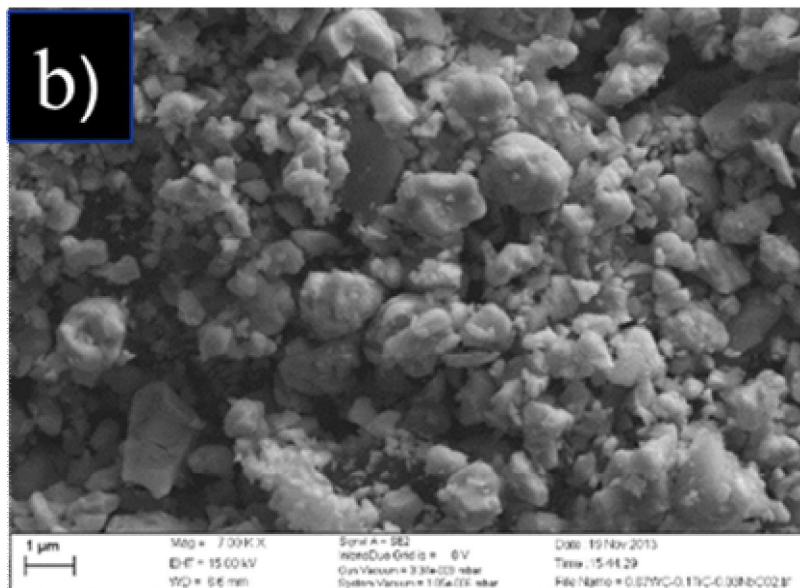
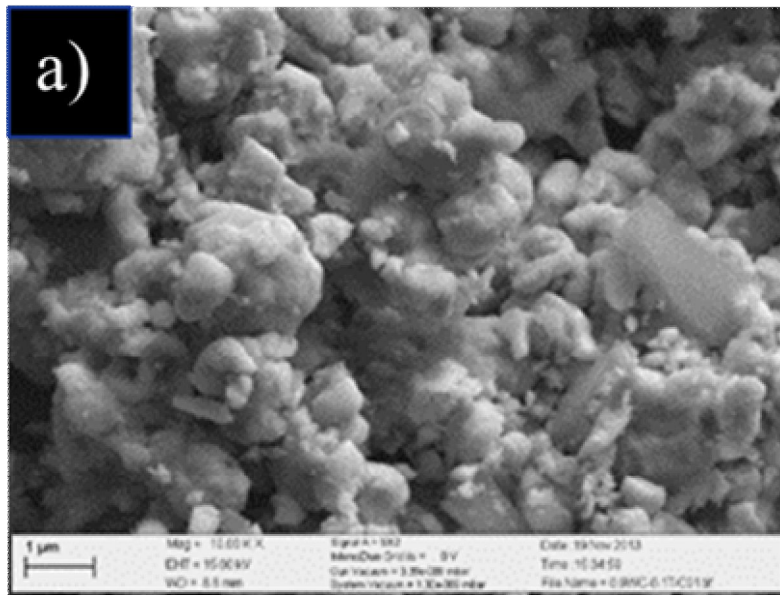


Fig 3. The SME micrograph of mixed powder via ball milling for 20 hours (a).WC-3.3TiC, (b). WC-3.3TiC-4.2NbC (conventionally fabricated)

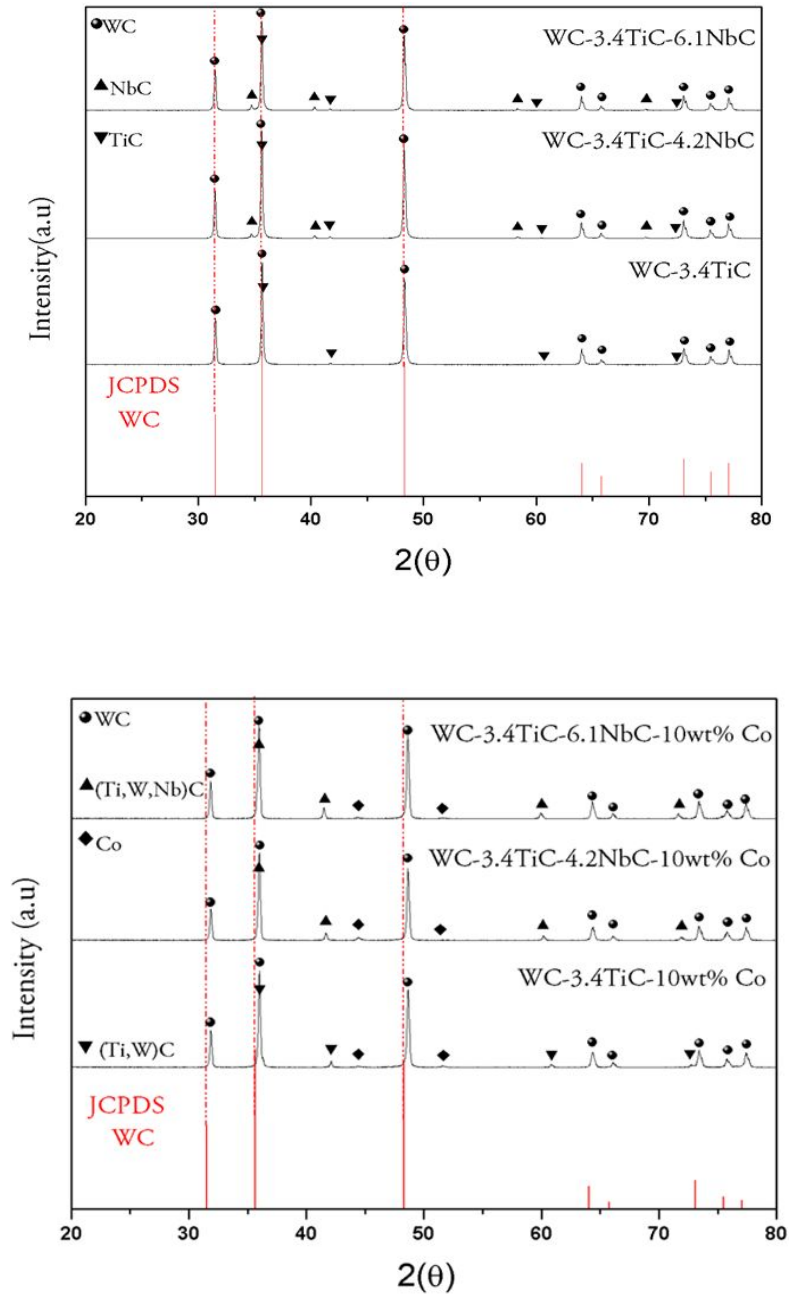


Fig 4. The XRD results of: mixed powder via ball milling (a)WC-3.4TiC, WC-3.4TiC-4.2NbC and (b)sintered specimens at 1450 °C for 1h WC-3.4TiC-10wt%Co, WC-3.4TiC-4.2NbC-10wt%Co and WC-3.4TiC-6.1NbC (conventional system)

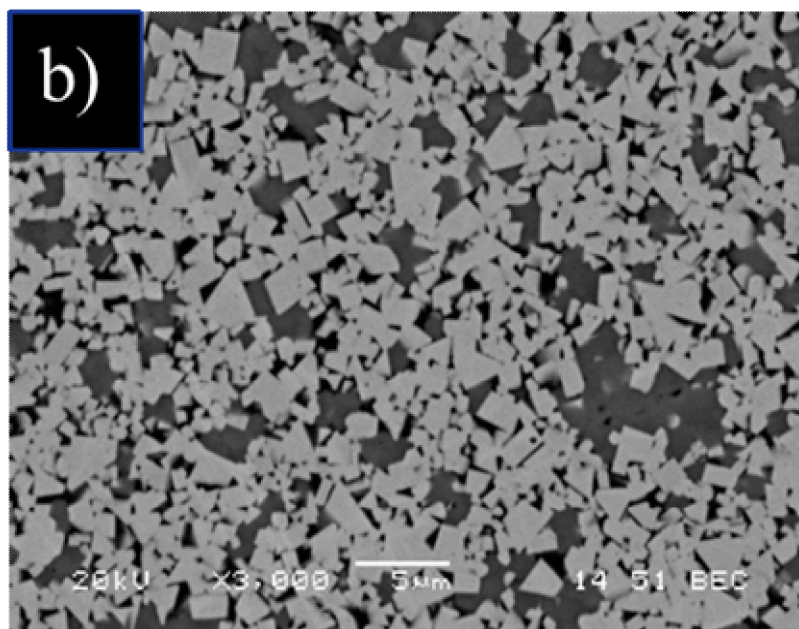
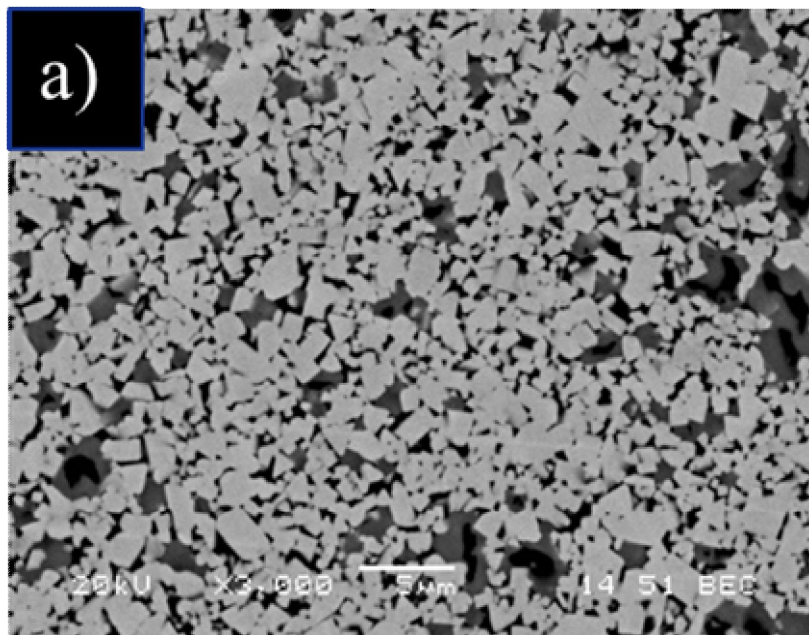


Fig 5. The SEM micrograph of sintered conventional samples (a). WC-3.4TiC-10wt%10Co, (b). WC-3.4TiC-4.2NbC-10wt%Co

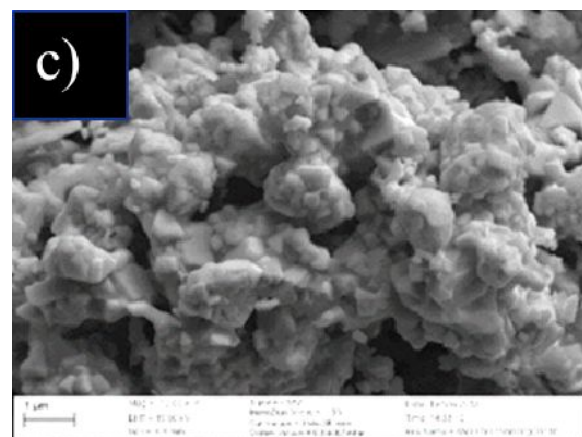
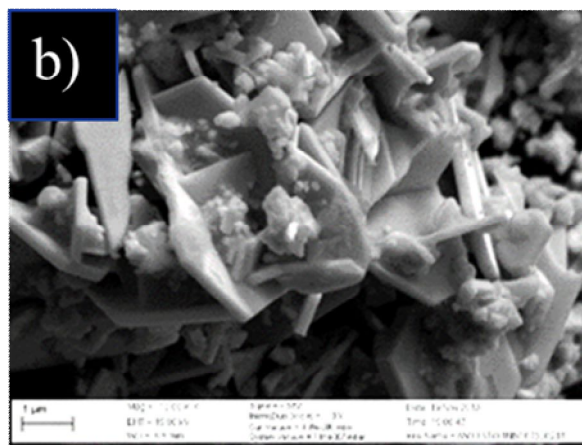
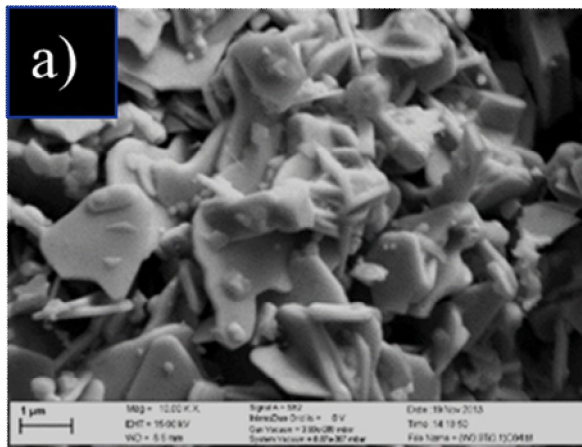


Fig 6. The SEM micrograph of reduced powder at 1400 °C for 2h in vacuum: (a).  $(W_{0.9}Ti_{0.1})C$ , (b).  $(W_{0.83}Ti_{0.1}Nb_{0.07})C$  and (c).  $(W_{0.8}Ti_{0.1}Nb_{0.1})C$



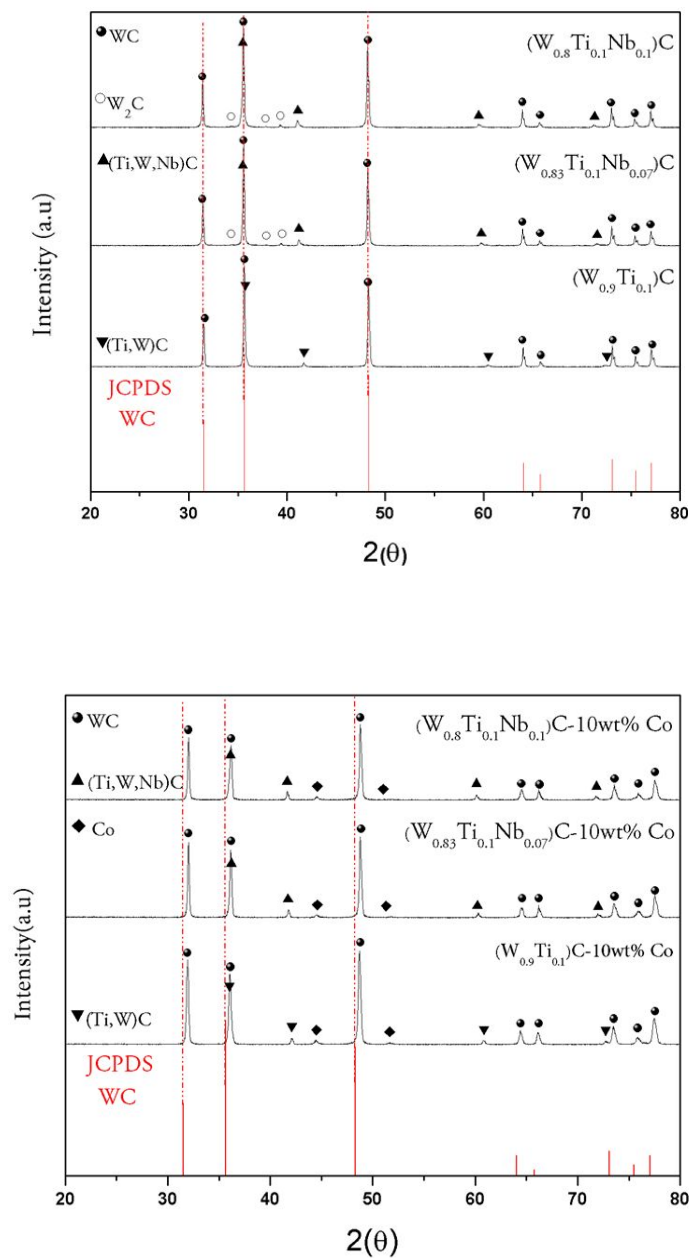


Fig 7. The XRD results of: reduced powder at 1400C for 2hours  $(W_{0.9}Ti_{0.1})C$ ,  $(W_{0.83}Ti_{0.1}Nb_{0.07})C$  &  $(W_{0.8}Ti_{0.1}Nb_{0.1})C$  and sintered specimens at 1450C for 1hou  $(W_{0.9}Ti_{0.1})C$ -10wt%Co,  $(W_{0.83}Ti_{0.1}Nb_{0.07})C$ -10wt%Co &  $(W_{0.8}Ti_{0.1}Nb_{0.1})C$ -10wt%Co

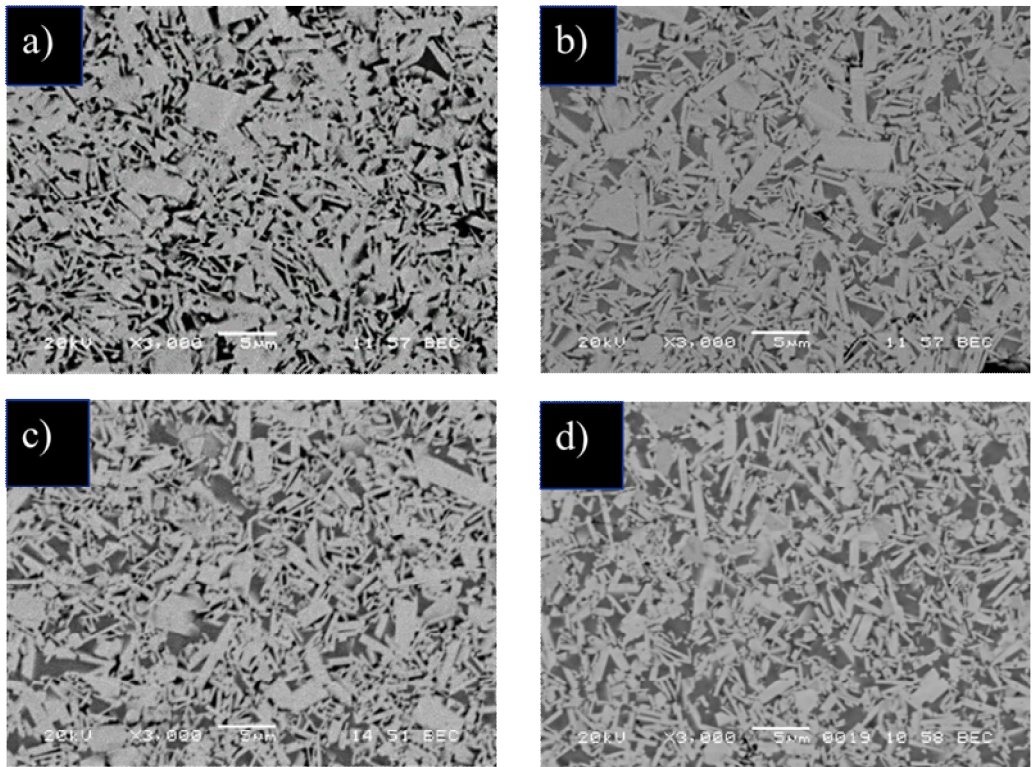


Fig 8. SEM micrograph of sintered specimens at 1450C for 1hour in vacuum  $(W_{0.9}Ti_{0.1})C-10wt\%Co$ ,  $(W_{0.83}Ti_{0.1}Nb_{0.07})C-10wt\%Co$  &  $(W_{0.8}Ti_{0.1}Nb_{0.1})C-10wt\%Co$

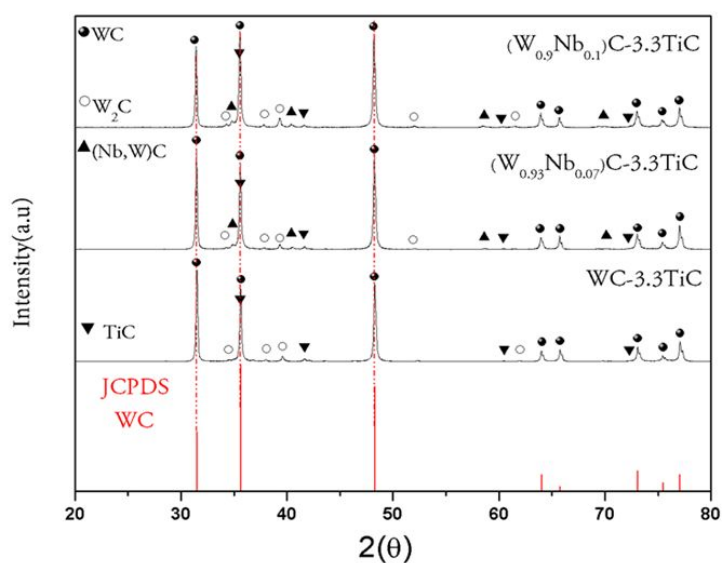
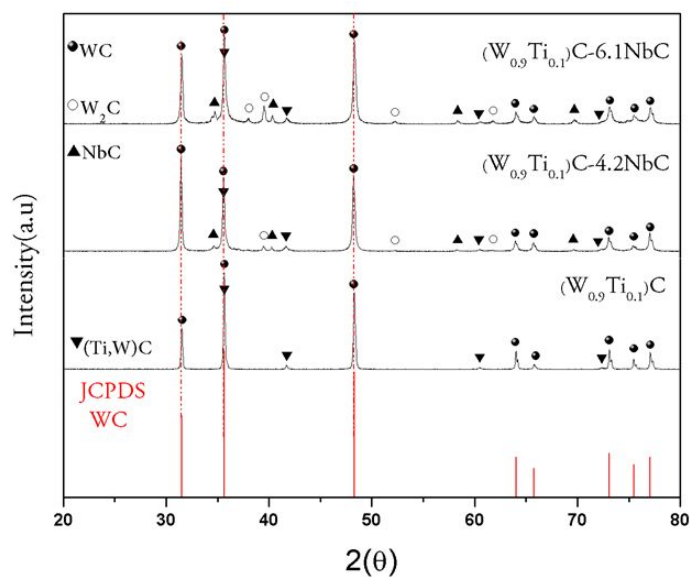


Fig 9. The XRD results of hybrid 1&2  $(W_{0.9}Ti_{0.1})C$ ,  $(W_{0.83}Ti_{0.1}Nb_{0.07})C$ ,  $(W_{0.8}Ti_{0.1}Nb_{0.1})C$  and  $WC-3.3TiC$ ,  $(W_{0.93}Nb_{0.07})C-3.3TiC$ ,  $(W_{0.9}Nb_{0.1})C-3.3TiC$  respectively



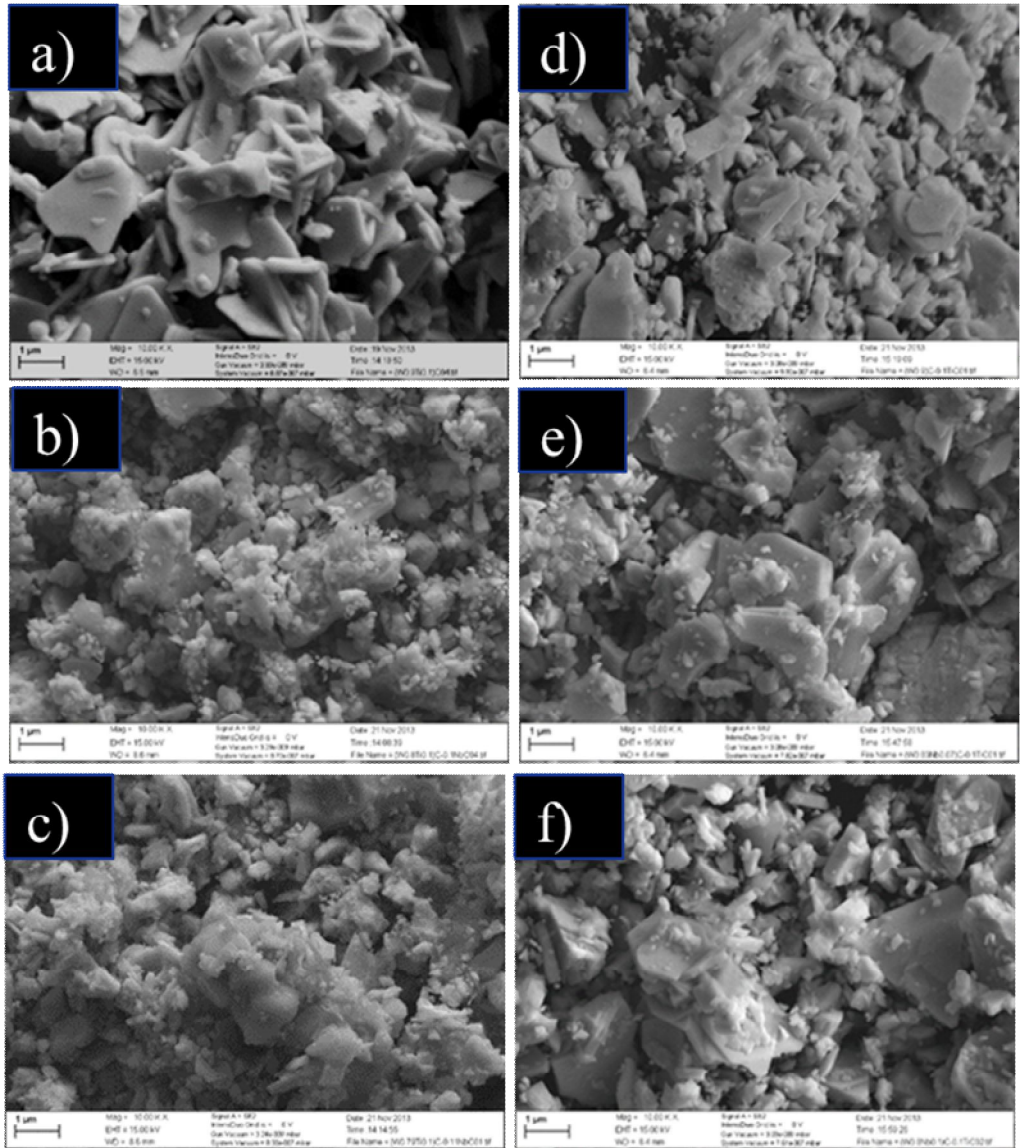


Fig 10. SEM micrograph of 1& 2 mixed powders via ball milling: (a).  $(W_{0.9}Ti_{0.1})C$ , (b).  $(W_{0.9}Ti_{0.1})C-4.2NbC$ , (c).  $(W_{0.9}Ti_{0.1})C-6.1NbC$ , (d).  $WC-3.3TiC$ , (e).  $(W_{0.93}Nb_{0.07})C-3.3TiC$ , (f).  $(W_{0.9}Nb_{0.1})C-3.3TiC$

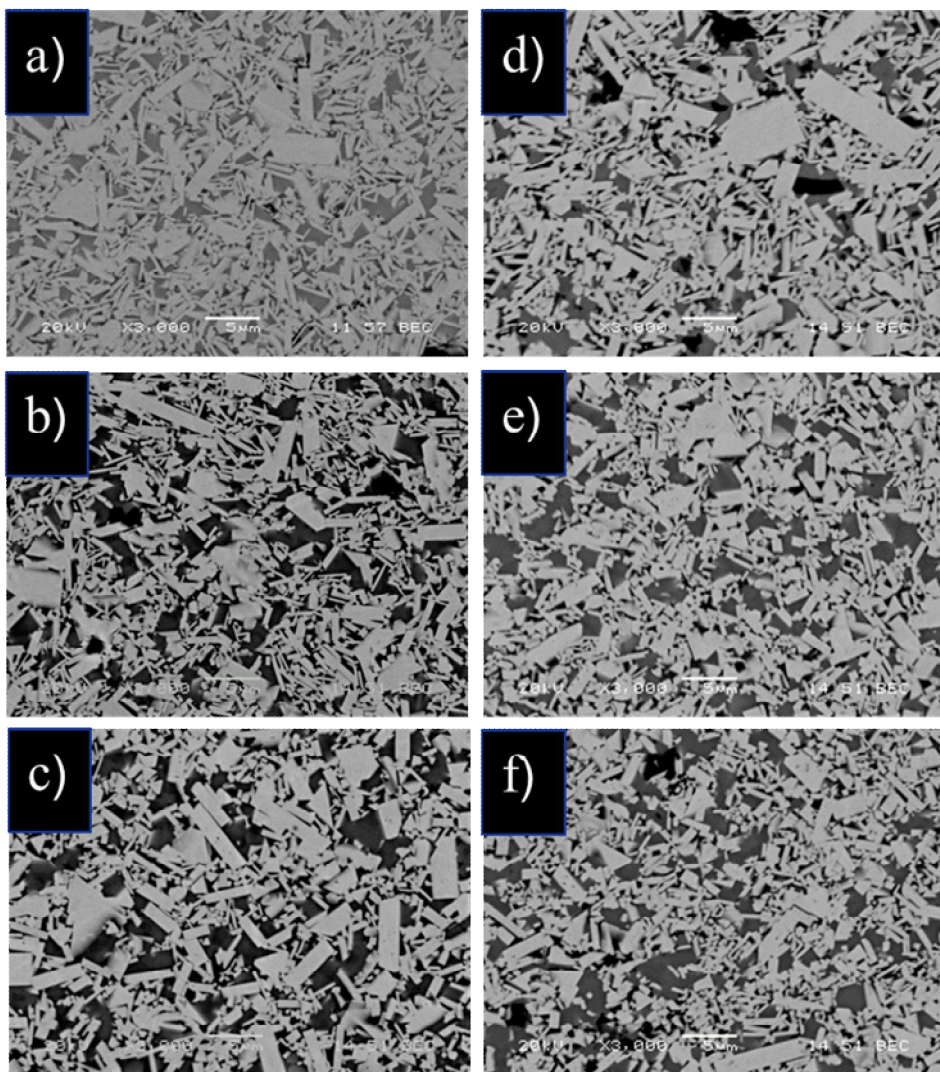


Fig 11. The SEM micrograph of hybrid 1& 2 sintered specimens  
 (a).( $W_{0.9}Ti_{0.1}$ )C-10wt%Co, (b).( $W_{0.9}Ti_{0.1}$ )C-4.2NbC-10wt%Co, (c).  
 ( $W_{0.9}Ti_{0.1}$ )C-6.1NbC-10wt%Co, (d).WC-3.3TiC-10wt%Co,  
 (e).( $W_{0.93}Nb_{0.07}$ )C-3.3TiC-10wt%Co, (f).( $W_{0.9}Nb_{0.1}$ )C-3.3TiC-  
 10wt%Co

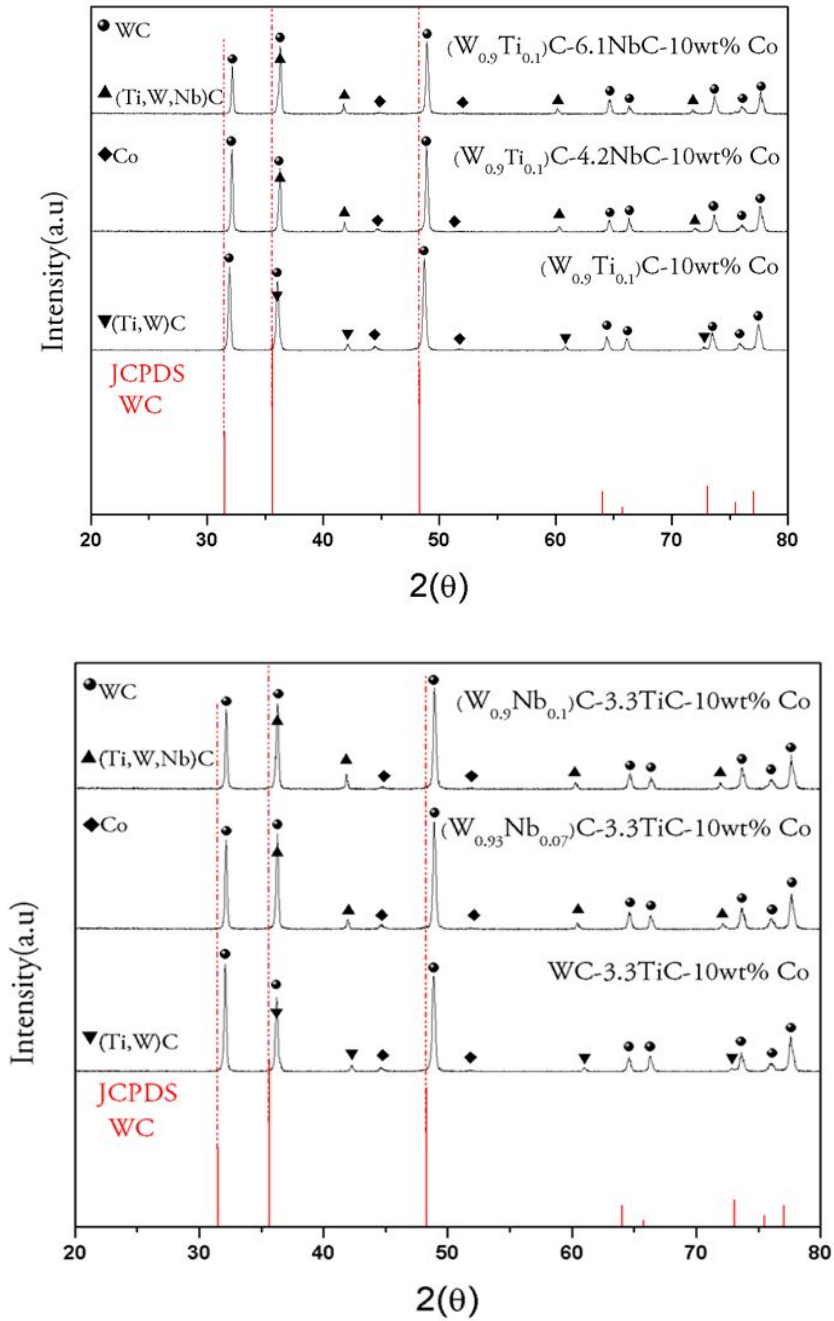


Fig 12. XRD results of hybrid 1 & 2 sintered specimens:  $(W_{0.9}Ti_{0.1})C$ -10wt%Co,  $(W_{0.9}Ti_{0.1})C$ -4.2NbC-10wt%Co,  $(W_{0.9}Ti_{0.1})C$ -6.1NbC-10wt%Co, WC-3.3TiC-10wt%Co,  $(W_{0.93}Nb_{0.07})C$ -3.3TiC-10wt%Co,  $(W_{0.9}Nb_{0.1})C$ -3.3TiC-10wt%Co

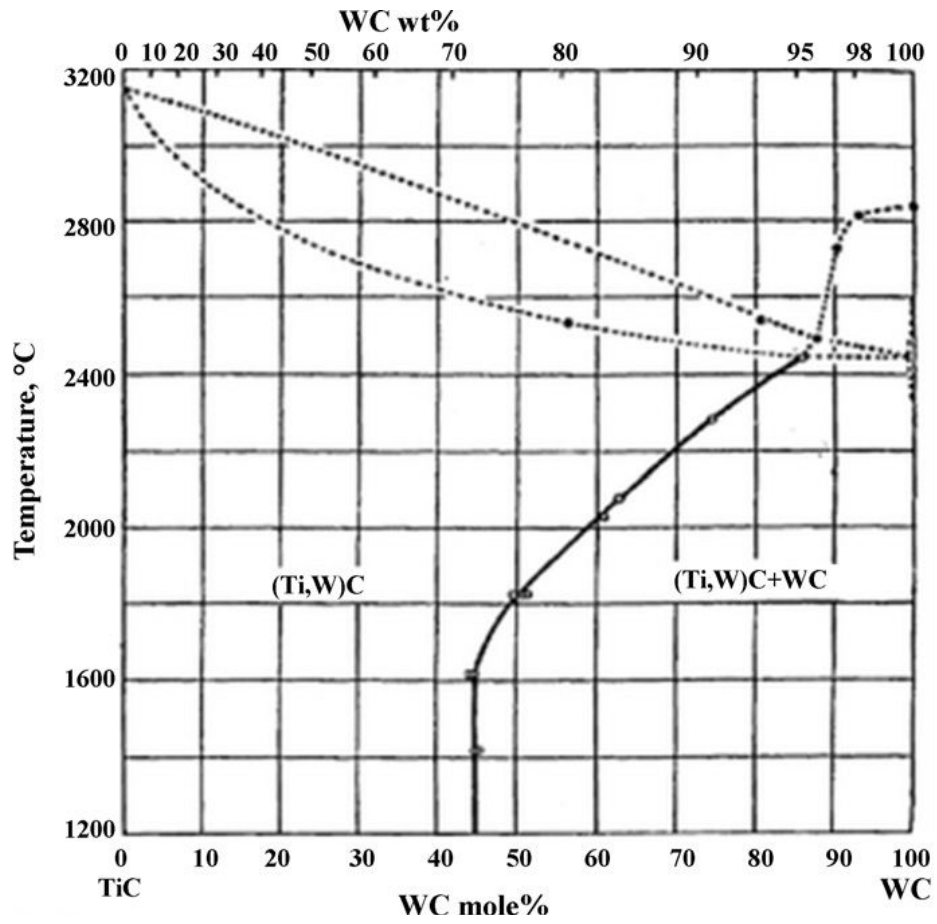


Figure 13. The binary phase diagram of WC–TiC[7]

# Abstract

## 한국어 제목

Pathou Badibanga

Department of Material Science and Engineering

The Graduate School

Seoul National University

### The Microstructural and Mechanical Properties of Platelet (W, M1, M2) C-Co Ternary System

WC-Co cemented carbides are widely used as the material in making cutting tools due to their superior wear resistance, hardness, and toughness. The WC particles that are embedded on the cobalt binder are grown by Ostwald ripening during liquid phase sintering. It has been found that the morphology of WC particles in the cobalt binder consists of platelets, a feature which enhances the material's toughness by deterring crack propagation. By controlling the high energy ball milling, the temperature during reduction, the addition of TiC, the nano effects, and so forth, one can observe the formation of platelet WC.

Until now, the most successful way of controlling the growth of WC grain is with the addition of small amounts of WC grain growth inhibitors. Our previous research on the microstructure evolution of the WC platelet, tungsten carbide particles demonstrated that the morphology, size, and mechanical properties of WC-Co cermets change significantly with the addition of

transitional metals such as titanium carbide (TiC), vanadium carbide (VC), and chromium carbide (Cr<sub>2</sub>C<sub>3</sub>). Especially in case of TiC, (W,Ti) C-phase was found to have formed with a thin, platelet morphology, enhancing the toughness of the (W,Ti) C-Co cermets.

The purpose of this research was to enhance the hardness of the material by controlling the size and morphology of WC platelets and by maintaining the same toughness for different systems with the addition of NbC to the initial, binary WC-Co system.

In this research, four different ternary systems (such as in-situ, hybrid one and two, and conventional) were prepared using TiC and NbC to control the size and morphology of tungsten carbide platelets. The mole fraction of TiC was fixed at 0.1 in all of the systems, and the NbC mole fraction varied between 0.07 and 0.1 in all of the systems as well. The alloys that started with the oxide powder were produced via planetary milling, and those that started with carbide powder were prepared through ball milling, then all of the systems were sintered at 1450°C for 1 hour. Analysis of the microstructure revealed that all of the systems contained WC platelets and that their aspect ratios had increased when TiC and NbC were added simultaneously. Thus, the addition of transitional metals was found to be effective in increasing the aspect ratios of the different systems that were studied in this research.

